

A theoretical study on the regioselectivity of 1,3-dipolar cycloadditions using DFT-based reactivity indexes

M. José Aurell,^a Luis R. Domingo,^{a,*} Patricia Pérez^b and Renato Contreras^{c,*}

^aDepartamento de Química Orgánica, Instituto de Ciencia Molecular, Universidad de Valencia, Dr. Moliner 50, 46100 Burjassot, Valencia, Spain

^bDepartamento de Ciencias Químicas, Facultad de Ecología y Recursos Naturales, Universidad Nacional Andrés Bello, República 275, Santiago, Chile

^cDepartamento de Química, Facultad de Ciencias, Universidad de Chile, Casilla 653, Santiago, Chile

Abstract—The regioselectivity for a series of four 1,3-dipolar cycloaddition reactions has been studied using global and local reactivity indexes. The results of the theoretical analysis suggest that for asynchronous cycloadditions associated to polar processes, the regioselectivity is consistently explained by the most favorable two-center interactions between the highest nucleophilic and electrophilic sites of the reagents.

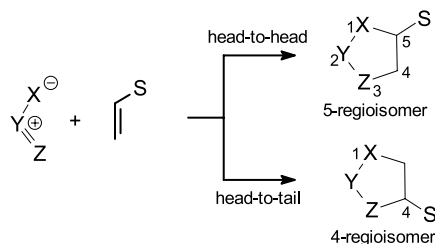
1. Introduction

Cycloaddition reactions are one of the most important processes with both synthetic and mechanistic interest in organic chemistry. Current understanding of the underlying principles in the Diels–Alder (DA) and the 1,3-dipolar cycloaddition (13DC) reactions has grown from a fruitful interplay between theory and experiment.¹ The usefulness of these cycloaddition reactions arises from their versatility and from their remarkable stereochemistry.² By varying the nature of the reagents many different types of carbocyclic structures can be built up. The interaction between

unsymmetrical reagents in a 13DC reaction can give two isomeric adducts depending on the relative position of the substituent in the cycloadduct, head-to-head, 5-regioisomer, or head-to-tail, 4-regioisomer (see Scheme 1).

It is well known that one of the preferred theoretical devices of synthetic organic chemists to discuss reactivity and selectivity of many organic reactions is the frontier molecular orbital (FMO) model introduced by Fukui.³ In the case of cycloaddition reactions, there are several examples that illustrate well the usefulness of this approach to classifying the 13DC reactions.^{4–6} Within the FMO frame, selectivity is usually described in terms of the square of the FMO coefficients, or in other cases by this same term weighted by a resonance integral, a model proposed by Houk,⁶ based on the orbital control term in the Salem,⁷ Klopman,⁸ and other equations.

There is however some relationships between the FMO approach and the one framed on the density functional theory (DFT) based reactivity indexes.⁹ They are the following: (a) the square of the coefficients, which is used to describe positional selectivity in a molecule within the FMO model represents in DFT a good approximation to the Fukui functions condensed to atoms in their valence state;^{10,11} (b) the model using the square of the coefficients weighted by a resonance integral on the other hand, accounts for just a piece of the interaction energy between the dipole and the dipolarophile localized in specific regions



Regioisomeric pathways for a 1,3-dipolar cycloaddition

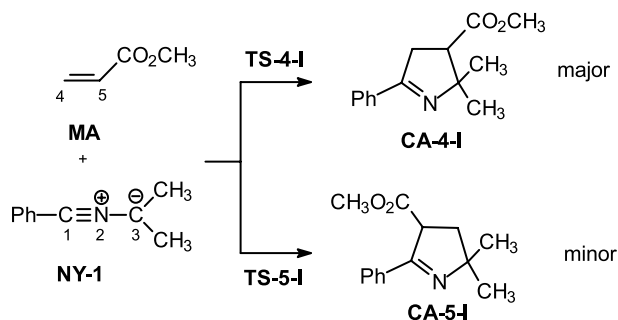
Scheme 1.

Keywords: 1,3-Dipolar cycloadditions; Regioselectivity; Local electrophilicity; Fukui functions; Density functional theory.

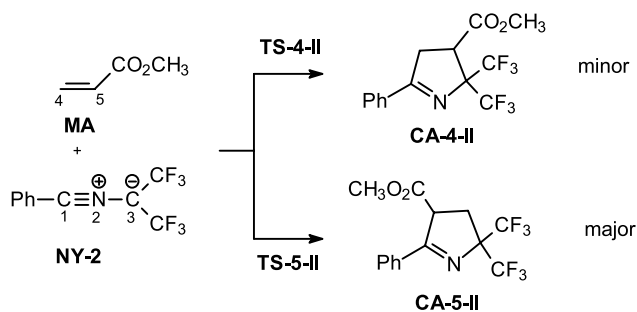
* Corresponding author. Tel.: +34 96 354 3106; fax: +34 96 354 3152; e-mail: domingo@utopia.uv.es

of the interacting pair, describing charge transfer stabilization effects in the FMO framework. Charge transfer may also be quantitatively described within DFT in terms of the electronic chemical potential and the chemical hardness throughout Pearson's equations,¹² and also within the concept of global electrophilicity introduced by Parr et al.¹³ For instance, using the DFT reactivity model, the regioselectivity in the cycloaddition reactions has been described in terms of a local hard and soft acid and bases (HSAB) principle, and some empirical rules have been proposed to rationalize the experimental regioselectivity pattern observed in some DA¹⁴ and 13DC¹⁵ reactions. Recent DFT studies devoted to the DA¹⁶ and 13DC¹⁷ reactions on the other hand, have shown that the classification of reagents within a unique scale of electrophilicity, is a useful tool for predicting the reaction mechanism and regioselectivity of a cycloaddition process.¹⁶ Even though in the case of the 13DC reactions the global analysis resulted more complex, substitution effects on the dipole and dipolarophile were correctly assessed.¹⁷ In a DA reaction, diene/dienophile pairs located at the ends of the electrophilicity scale usually display a polar reactivity characterized by a large charge transfer (CT) at the transition structure (TS) involved in the mechanism of this particular cycloaddition reaction.^{16a} For these polar cycloadditions the most favorable regioisomeric pathway corresponds to the bond-formation at the more electrophilic and nucleophilic sites of unsymmetrical reagents. In this context, we have shown that the analysis based on the local electrophilicity index ω_k ,¹⁸ at the more electrophile DA reagent together with the analysis of the nucleophilic Fukui functions,¹⁹ f_k^- , at the less electrophilic one, allows the prediction of the regioselectivity in these cycloadditions.^{16c-g}

There is not a single criterion however to explain most of the experimental evidence accumulated in cycloaddition



Scheme 2.



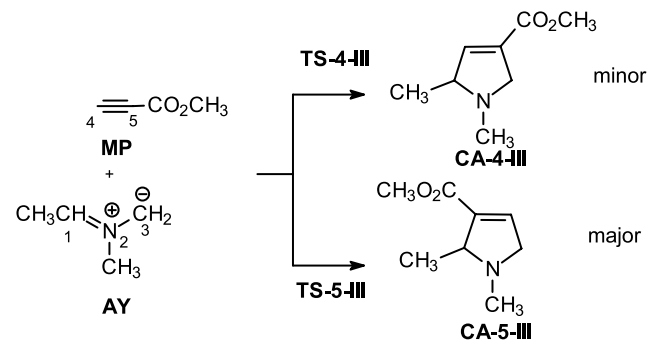
Scheme 3.

processes involving four center interactions. Recent studies devoted to regioselective 13DC reactions have questioned the feasibility of the FMO approach to explain this kind of selectivity.²⁰ An excellent source for the discussion of regioselectivity in concerted pericyclic reactions is given in reference.^{15d} In this context, the model based on DFT global and local descriptors is a reliable alternative to discuss reactivity and selectivity based on absolute scales, which have been already validated against experimental scales of reactivity and selectivity.

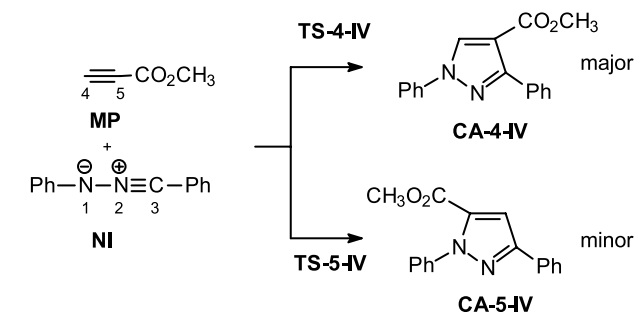
In this work we extend the local analysis to the regioselectivity of the 13DC processes. We have chosen as model reactions a series of four regioselective 13DC reactions for which experimental data are available. They are the reactions between the nitrile ylides NY-1^{1d} and NY-2²¹ with methyl acrylate (MA), models I and II in Schemes 2 and 3, and the 13DC reactions of the azomethine ylide AY²² and the nitrile imine NI²³ with methyl propiolate (MP), models III and IV in Schemes 4 and 5, respectively. The comparative analysis will be made on the basis of the relative energies, asynchronicity and CT at the TSs on one hand, and the analysis based on the reactivity indexes defined in the context of DFT^{9c} evaluated at the ground state (GS) of reactants.

2. Computational methods and models

In recent years, theoretical methods based on the DFT have emerged as an alternative to traditional ab initio methods in the study of structure and reactivity of chemical systems. DA and 13DC reactions have been the object of several DFT studies showing that functionals that include gradient corrections and hybrid functionals for exchange and correlation, such as B3LYP,²⁴ together with the standard



Scheme 4.



Scheme 5.

6-31G* basis set,²⁵ yield potential energy barriers in good agreement with the experiment.²⁶ Thus, in the present study geometrical optimizations of the stationary points were carried out using this methodology. The optimizations were performed using the Berny analytical gradient optimization method.²⁷ The stationary points were characterized by frequency calculations in order to verify that the TSs had one and only one imaginary frequency. The intrinsic reaction coordinate (IRC)²⁸ path was traced in order to check the energy profiles connecting each TS to the two associated minima of the proposed mechanism by using the second order González–Schlegel integration method.²⁹ The electronic structures of TSs were analyzed by the natural bond orbital (NBO) method.³⁰ All calculations were carried out using the Gaussian 98 suite of programs.³¹ Thermal corrections to enthalpy and entropy values were evaluated at 298.15 K. The computed values of enthalpies, entropies and free energies were estimated by means of the B3LYP/6-31G* potential energy barriers, along with the gas-phase harmonic frequencies.²⁵

The global electrophilicity index ω ,¹³ which measures the stabilization in energy when the system acquires an additional electronic charge ΔN from the environment, has been given the following simple expression,¹³ $\omega = (\mu^2/2\eta)$, in terms of the electronic chemical potential μ and the chemical hardness η . Both quantities may be approached in terms of the one electron energies of the frontier molecular orbital HOMO and LUMO, ε_H and ε_L , as $\mu \approx (\varepsilon_H + \varepsilon_L)/2$ and $\eta \approx (\varepsilon_L - \varepsilon_H)$, respectively.³²

The local electrophilicity index, ω_k ,¹⁸ can be expressed as $\omega_k = \omega f_k^+$ where f_k^+ is the Fukui function for a nucleophilic attack. This expression shows that the maximum electrophilicity power in a molecule will be developed at the site where the Fukui function for a nucleophilic attack displays its maximum value, i.e. at the active site of the electrophile. Electrophilic and nucleophilic Fukui functions³² condensed to atoms have been evaluated from single point calculations performed at the GS of molecules at the same level of

theory, using a method described elsewhere.¹¹ This method evaluates the Fukui functions using the coefficients of the frontier molecular orbitals involved in the reaction and the overlap matrix.

3. Results and discussion

We first evaluated the activation energies and the geometrical parameters of TSs for the four 13DC reactions. The population analysis at the TSs in terms of bond orders and natural charges was performed, together with an analysis based on the global and local reactivity indexes of the reactants involved in these cycloadditions.

3.1. Analysis of activation energies, geometries, bond orders, and charge transfer at the transition state geometries

An analysis of the gas-phase results indicates that these 13DC reactions take place along asynchronous concerted processes. Therefore eight TSs, **TS-4-I**, **TS-5-I**, **TS-4-II**, **TS-5-II**, **TS-4-III**, **TS-5-III**, **TS-4-IV** and **TS-5-IV**, and their corresponding cycloadducts associated with the two regioisomeric channels of the four cycloadditions were located and characterized. These acronyms are related to the formation of the 4- or 5-regioisomers, hereafter structures **4** and **5**, the 13DCs between **NY-1** and **MA**, named model **I**, the cycloaddition between **NY-2** and **MA**, named model **II**, the cycloaddition between **AY** and **MP**, named model **III**, and the cycloaddition between **NI** and **MP**, named model **IV**. The stationary points corresponding to these 13DC reactions are presented in Schemes 2–5 together with atom numbering. The total and relative energies are compiled in Table 1. The geometries of the TSs are presented in Figure 1.

These 13DC reactions present very low activation enthalpies. For instance, for the reaction model **III**, **TS-5-III** is located 7.6 kcal/mol below the reactants. However,

Table 1. Relative^a energies (ΔE , in kcal/mol), enthalpies (ΔH , in kcal/mol), entropies (ΔS , in kcal/mol K) and free energies (ΔG , in kcal/mol) energies computed at 25 °C of the stationary points involved in the 13DC reaction models **I–IV**

	ΔE	ΔH	ΔS	ΔG
Model I (NY-1 + MA)				
TS-4-I	1.04	0.72	−43.97	13.83
TS-5-I	3.20	2.66	−48.30	17.06
CA-4-I	−58.76	−60.20	−55.60	−43.62
CA-5-I	−57.57	−59.05	−56.09	−42.33
Model II (NY-2 + MA)				
TS-4-II	1.75	1.72	−46.06	15.45
TS-5-II	1.52	1.41	−47.83	15.67
CA-4-II	−60.56	−61.52	−57.79	−44.29
CA-5-II	−61.25	−62.20	−56.35	−45.40
Model III (AY + MP)				
TS-4-III	−6.41	−6.48	−39.08	5.18
TS-5-III	−7.57	−7.67	−40.48	4.40
CA-4-III	−87.29	−88.45	−48.48	−74.00
CA-5-III	−86.96	−88.16	−48.88	−73.58
Model IV (NI + MP)				
TS-4-IV	6.08	5.75	−44.64	19.06
TS-5-IV	5.74	5.47	−44.12	18.63
CA-4-IV	−98.65	−100.07	−55.61	−83.50
CA-5-IV	−96.93	−98.28	−53.93	−82.20

^a Relative to the corresponding reagents.

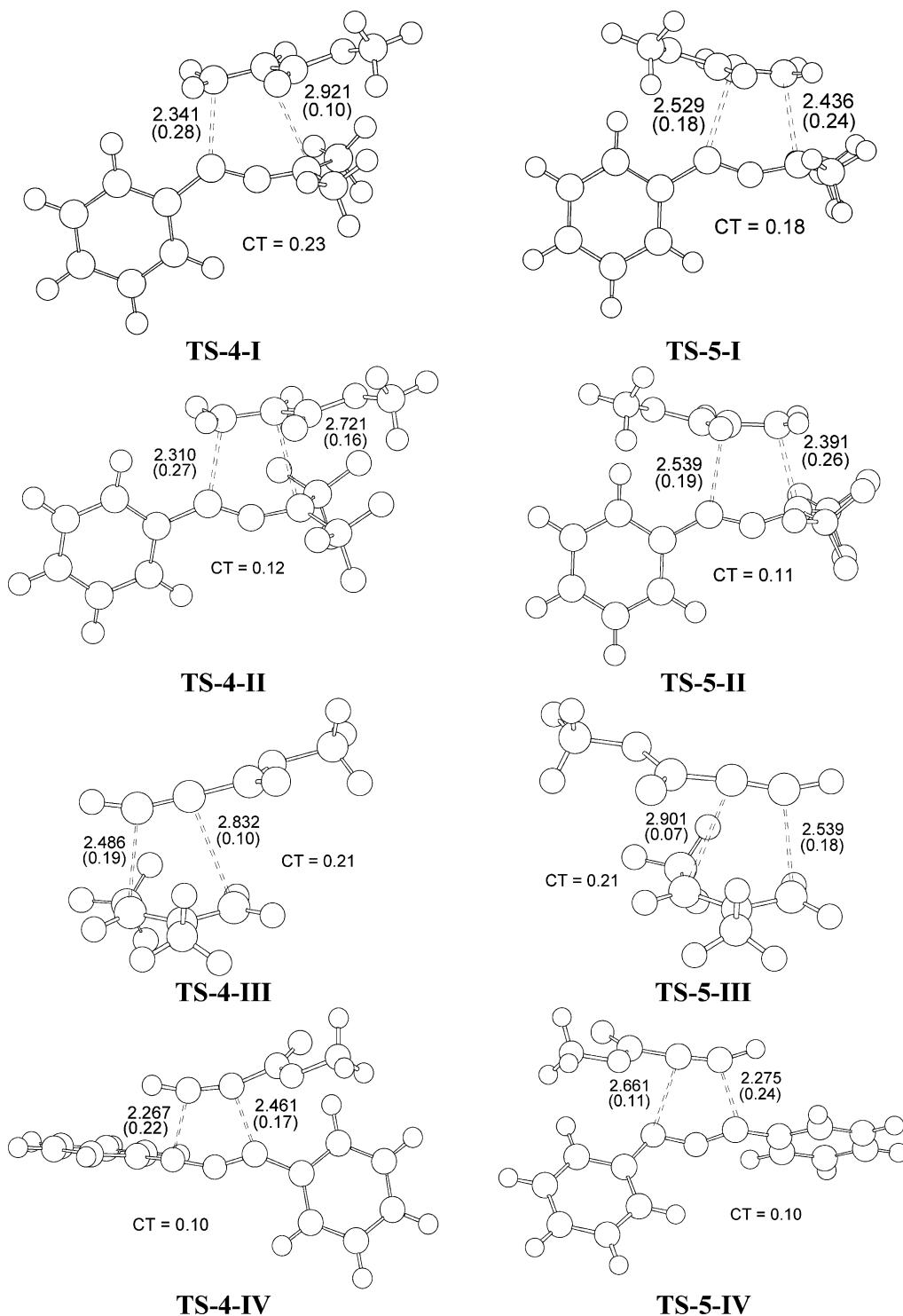


Figure 1. Transition structures corresponding to the regioisomeric path of the 13DC reaction models I-IV. The bond lengths directly involved in the reaction are given in angstroms. The bond orders are given in parenthesis. The charge transfers (CT) are given in a.u.

inclusion of the activation entropies to the free energies brings the activation free energy associated to **TS-5-III** to 4.4 kcal/mol. These cycloadditions are very exothermic by about -60 to -100 kcal/mol. The analysis of the regioselectivity for these 13DC reactions measured as the difference of activation enthalpies between the TSs leading to different regioisomers shows that they fall in a narrow range between 0.3 and 1.9 kcal/mol. While for the reaction models **I**, **II** and **III** the B3LYP/6-31G* calculations predict

the regioselectivity experimentally observed, for the model **IV** it fails. Furthermore, previous theoretical studies on 13DC reactions have pointed out that the regioselectivity of this type of cycloadditions is strongly dependent on the computational level used.³³

An analysis of the geometries at the TSs given in **Figure 1** indicates that they correspond to asynchronous bond-formation processes. While for the reaction models **I**, **III**

and **IV** the more asynchronous TSs correspond to less energetic one, **TS-4-I**, **TS-5-III** and **TS-5-IV**, for model **II** the result is different. In this case, the hindrance that appears between the carboxylate group present in **MA** and the two trifluoromethyl groups present in the dipole **NY-2** may account for the large asynchronicity found at **TS-4-II**.

The extent of bond-formation along a reaction pathway may be provided by the quantitative concept of bond order (BO).³⁴ The BO values of the C–C and N–C σ -bond that are being formed along these 13DC reactions are shown in parenthesis in Figure 1. These values are within the range of 0.07 to 0.28. Therefore, it may be suggested that these TSs correspond to early processes. In general, the asynchronicity shown by the geometrical data is accounted for by the BO values. The reaction models **I** and **III**, which present larger regioselectivity, also present the more asynchronous TSs along the more favorable reactive channels **TS-4-I** and **TS-5-III**, respectively.

Finally, the CT was evaluated at the corresponding TSs. The natural charges at the TSs appear shared between the dipole framework, **NY-1**, **NY-2**, **AY** and **NI**, and the dipolarophile moiety, **MA** and **MP**, respectively. The resulting values are presented in Figure 1. The CT ranges from 0.10 e for model **IV** to 0.23 e for model **I**. For all cases the CT flows from the dipole to the dipolarophile. For models **II–IV** both regioisomeric TSs present the same CT pattern. Only model **I** presents a larger charge transfer at the more favorable reactive channel; 0.23 e at **TS-4-I** compared to 0.18 e at **TS-5-I**.

3.2. Analysis based on the global and local electrophilicity at the ground state of reagents

In Table 2 are displayed the electronic chemical potential μ , chemical hardness η , global electrophilicity ω . Also included in Table 2 are the values of local electrophilicity and the electrophilic and nucleophilic Fukui functions for the dipoles **NY-1**, **NY-2**, **AY** and **NI**, and the dipolarophiles **MA** and **MP**. The electronic chemical potential, μ , of the four dipoles with values between -0.0585 a.u. and -0.1408 a.u., are higher than those for the dipolarophiles **MA** and **MP**, -0.1586 a.u. and -0.1624 a.u., respectively. Therefore the CT at these 13DC reactions will take place from the dipole to the dipolarophile, in complete agreement with the CT analysis performed at the TSs (see Section 3.1). The two dipolarophiles present similar electrophilicity values, 1.51 eV (**MA**) and 1.52 eV (**MP**). According to the absolute scale of electrophilicity based on the ω index,^{16a} these compounds may be classified as strong electrophiles. On the other hand, the four dipoles present electrophilicity values in a wider range: 0.31 eV for **AY**, 1.15 eV for **NY-1**, 1.43 eV for **NI** and 1.95 eV for **NY-2**. Thus, while **AY** is classified as a marginal electrophile (and probably a good nucleophile), **NY-2** is classified as a strong electrophile. Note that even though **NY-2** presents a larger electrophilicity value than **MA**, the later has a lower chemical potential, which is the index that determines the direction of the electronic flux along the cycloaddition. Therefore, along this series of 13DC reactions the more favorable interaction will take place between the less electrophilic specie, **AY**, namely the dipoles in the present

case, and the electrophilic dipolarophile **MP**. Note that for the 13DC reaction between **AY** and **MP**, **TS-4-III** and **TS-5-III** are located below reactants on potential energy surface. In addition, the lower CT found for models **II** and **IV** can be related to the similar electrophilicity values displayed by the dipoles and dipolarophiles (see Table 2). In these cases, along the cycloaddition pathway any of them have the same trend to supply or accept electron density from each other.

Recent studies devoted to regioselective DA reactions have shown that the analysis of the local electrophilicity,¹⁸ ω_k , at the electrophile together with the analysis of the nucleophilic Fukui functions, f_k^- ,¹⁹ at the nucleophile, allows the prediction of the regioselectivity in these competitive cycloadditions.^{16b,c,g} The local functions are also summarized in Table 2. For the two dipolarophiles **MA** and **MP**, classified as strong electrophiles, the C4 carbon atom (the β -position) presents a larger local electrophilicity value than the C5 site.³⁵ Therefore, the C4 will be the preferred position for a nucleophilic attack by a dipole. This fact is in agreement with the asynchronicity shown at all the TSs. The C(N)1–C4 or C(N)3–C4 bonds formed at **TS-4-X** or **TS-5-X**, respectively, are shorter and more advanced than the C(N)3–C5 or C(N)1–C5 ones. This fact that has also been observed in other cycloaddition reactions suggests that the most electrophilic reagents control the asynchronicity of the process by a larger bond-formation process at the most electrophilic site of the molecule.

A different local picture is found for the four dipoles where the values of the nucleophilic Fukui functions, f_k^- depend on both the structure of the dipole and the substitution pattern. For instance, for the nitrile ylide **NY-1** the C1 carbon atom has a larger f_k^- value than the C3 one, 0.53 and 0.29, respectively, while for the nitrile ylide **NY-2** there is a change on the local activation: now the C3 carbon atom presents the larger f_k^- value (see Table 2). This result allows to explain the change of regioselectivity for these 13DC reactions. Substitution of the two electron-releasing methyl groups present in **NY-1** by two electron-withdrawing CF_3 groups in **NY-2** produces a change in the polarization of the $\text{HOMO}_{\text{dipole}}$ which acts as a nucleophile, thereby reverting the regioselectivity pattern.

For the azomethyne ylide **AY**, the presence of the electron-releasing methyl group on the C1 position polarizes the $\text{HOMO}_{\text{dipole}}$ through the C3 carbon atom. As a result, the unsubstituted C3 carbon atom presents a larger f_k^- value compared to that at the C1 site. Therefore, along the cycloaddition reaction the more favorable reactive channel takes place through the C3–C4 bond-formation by the nucleophilic attack of the C3 carbon atom of **AY** to the more electrophilic C4 site of **MP**. Note that at the highly asynchronous **TS-5-III** the covalent interactions between the C1 and C5 are negligible.

Finally, for the 1,3-diphenylnitrile imine **NI** the N1 nitrogen atom presents a larger nucleophilic activation than the C3 carbon atom (see Table 2). Therefore, the local analysis predicts a more favorable interaction between the N1 nitrogen of **NI** and the C4 carbon atom of **MP** along the **TS-4-IV**, in agreement with the regioselectivity

Table 2. Global and local properties of dipoles **NY-1**, **NY-2**, **NI** and **AY** and dipolarophiles **MA** and **MP**. *k* defines de site in the molecule where the property is being evaluated

	Global properties					Local properties			
	HOMO	LUMO	μ (a.u.)	η (a.u.)	ω (eV)	<i>k</i>	f^+	f^-	ω_k (eV)
NY-2	-0.2097	-0.0718	-0.1408	0.1379	1.95	1	0.1819	0.2232	0.36
						2	0.1452	0.0160	0.28
						3	0.0714	0.4488	0.14
MP	-0.2806	-0.0442	-0.1624	0.2363	1.52	4	0.3055	0.2328	0.46
						5	0.1168	0.1655	0.18
MA	-0.2720	-0.0452	-0.1586	0.2268	1.51	4	0.4154	0.0048	0.62
						5	0.1969	0.0714	0.29
NI	-0.1827	-0.0520	-0.1173	0.1307	1.43	1	0.0759	0.2685	0.11
						2	0.1159	0.0104	0.17
						3	0.0662	0.1613	0.10
NY-1	-0.1771	-0.0392	-0.1081	0.1379	1.15	1	0.2100	0.5339	0.24
						2	0.1208	0.0274	0.14
						3	0.0089	0.2909	0.01
AY	-0.1341	0.0171	-0.0585	0.1512	0.31	1	0.3165	0.4379	0.10
						2	0.2481	0.0118	0.08
						3	0.3460	0.4937	0.11

experimentally observed. Note that the analysis based on the energetic results predicts a reverse regioselectivity.

In summary, the present model based on the local electrophilicity index appears as a reliable approach to discuss regioselectivity. For instance, electrophilic activation/deactivation promoted by chemical substitution is correctly assessed within this framework. All this information is easily available from the properties of the GS electron density, and its first derivative with respect to the number of electrons which defines the Fukui function of the system. The electrophilic Fukui function in turn, permits the projection of the global electrophilicity into atoms, or group of atoms (i.e. functional groups) in the molecule. The polarization pattern at the dipoles induced by substituent effects may be assessed from a static model based on the difference in electrophilicity of the dipole/dipolarophile interacting pair.

4. Conclusions

The regioselectivity for a series of four 13DC reactions has been studied using DFT methods at the B3LYP/6-31G* level. The analysis of the activation enthalpies, asynchronicity and charge transfer at the TSs, as well as the analysis of the global and local electrophilicity index at the GS of reactants have been performed in order to rationalize the regioselectivity experimentally observed in these cycloadditions. We found that for this series of 13DCs the observed regioselectivity is well explained by reactivity analysis performed using global and local electrophilicity indexes. While the analysis of the global indexes allows to anticipate the polar character of the reaction as well the shift of the CT along the cycloaddition process, the local analysis allows to identify the more electrophilic and nucleophilic centers of the two reactants. Along an asynchronous cycloaddition associated to a polar process the most favorable two-center interaction between the highest nucleophilic and electrophilic sites of the reagents is responsible for the regioselectivity observed on these 13DC reactions.

Acknowledgements

Work supported by Ministerio de Ciencia y Tecnología of the Spanish Government by DGICYT, project BQU2002-01032, the Agencia Valenciana de Ciencia y Tecnología of the Generalitat Valenciana, reference GRUPOS03/176, Fondecyt, grants N° 1030548 and 1020069, project DI-12-02 from Universidad Andres Bello, and Millennium Nucleus for Applied Quantum Mechanics and Computational Chemistry, grant N° P02-004-F from MIDEPLAN (Chile). L.R.D. thanks the Fondecyt grant N° 7030116 for financial support and the Universidad de Chile for the warm hospitality.

References and notes

- (a) Wasserman, A. *Diels–Alder Reactions*; Elsevier: New York, 1965. (b) Fleming, I. *Frontier Orbitals and Organic Chemical Reactions*; Wiley: New York, 1976. (c) Padwa, A. In *1,3-Dipolar Cycloaddition Chemistry*; Wiley-Interscience: New York, 1984; Vol. 1–2. (d) Padwa, A. In *Comprehensive Organic Chemistry*; Pergamon: Oxford, 1991; Vol. 4.
- (a) Carruthers, W. *Some Modern Methods of Organic Synthesis*, 2nd ed.; Cambridge University Press: Cambridge, 1978. (b) Carruthers, W. *Cycloaddition Reactions in Organic Synthesis*; Pergamon: Oxford, 1990.
- (a) Fukui, K. *Acc. Chem. Res.* **1981**, *14*, 363. (b) Fukui, K. *Acc. Chem. Res.* **1971**, *4*, 57. (c) Fukui, K. *Molecular Orbitals in Chemistry, Physics, and Biology*; Academic: New York, 1964; p 525.
- Fleming, I. *Frontier Orbitals and Organic Chemical Reactions*; Wiley: Chichester, UK, 1976.
- (a) Sustmann, R. *Tetrahedron Lett.* **1971**, 2717. (b) Sustmann, R.; Trill, H. *Tetrahedron Lett.* **1972**, 4271. (c) Sustmann, R. *Pure Appl. Chem.* **1974**, *40*, 569.
- (a) Houk, K. N.; Sims, J.; Watts, C. R.; Luskus, L. J. *J. Am. Chem. Soc.* **1973**, *95*, 7301. (b) Houk, K. N.; Sims, J.; Duke, R. E. Jr.; Strozier, R. W.; George, J. K. *J. Am. Chem. Soc.* **1973**, *95*, 7287.
- Salem, L. *J. Am. Chem. Soc.* **1968**, *90*, 543.

8. Klopman, J. *J. Am. Chem. Soc.* **1968**, *90*, 223.
9. (a) Roy, R. K.; Pal, S.; Hirao, K. *J. Chem. Phys.* **1999**, *110*, 8236. (b) Pérez, P.; Toro-Labbé, A.; Aizman, A.; Contreras, R. *J. Org. Chem.* **2002**, *67*, 4748. (c) Geerlings, P.; De Proft, F.; Langenaeker, W. *Chem. Rev.* **2003**, *103*, 1793.
10. Senet, P. *J. Chem. Phys.* **1997**, *107*, 2516.
11. (a) Contreras, R.; Fuentealba, P.; Galván, M.; Pérez, P. *Chem. Phys. Lett.* **1999**, *304*, 405. (b) Fuentealba, P.; Pérez, P.; Contreras, R. *J. Chem. Phys.* **2000**, *113*, 2544.
12. Pearson, R. G. *Chemical Hardness*; Wiley-VCH: Weinheim, 1997.
13. Parr, R. G.; von Szentpaly, L.; Liu, S. *J. Am. Chem. Soc.* **1999**, *121*, 1922.
14. Damoun, S.; Van de Woude, G.; Méndez, F.; Geerlings, P. *J. Phys. Chem. A* **1997**, *101*, 886.
15. (a) Chandra, A. K.; Nguyen, M. T. *J. Phys. Chem. A* **1998**, *102*, 6181. (b) Chandra, A. K.; Michalak, A.; Nguyen, M. T.; Nalewajski, R. F. *J. Phys. Chem. A* **1998**, *102*, 10182. (c) Mendez, F.; Tamariz, J.; Geerlings, P. *J. Phys. Chem. A* **1998**, *102*, 6292. (d) Ponti, A. *J. Phys. Chem. A* **2000**, *104*, 8843.
16. (a) Domingo, L. R.; Aurell, M. J.; Pérez, P.; Contreras, R. *Tetrahedron* **2002**, *58*, 4417. (b) Domingo, L. R.; Asensio, A.; Arroyo, P. *J. Phys. Org. Chem.* **2002**, *15*, 660. (c) Domingo, L. R.; Arnó, M.; Contreras, R.; Pérez, P. *J. Phys. Chem. A* **2002**, *952*. (d) Domingo, L. R. *Tetrahedron* **2002**, *58*, 3765. (e) Domingo, L. R.; Aurell, M. J. *J. Org. Chem.* **2002**, *959*. (f) Domingo, L. R.; Aurell, M. J.; Pérez, P.; Contreras, R. *J. Org. Chem.* **2003**, *68*, 3884. (g) Domingo, L. R.; Andrés, J. *J. Org. Chem.* **2003**, *68*, 8662.
17. (a) Pérez, P.; Domingo, L. R.; Aurell, M. J.; Contreras, R. *Tetrahedron* **2003**, *59*, 3117. (b) Sáez, A.; Arno, M.; Domingo, L. R. *Tetrahedron* **2003**, *59*, 9167. (c) Domingo, L. R.; Picher, M. T. *Tetrahedron* **2004**, *60*, 5053.
18. Domingo, L. R.; Aurell, M. J.; Pérez, P.; Contreras, R. *J. Phys. Chem. A* **2002**, *106*, 6871.
19. Parr, R. G.; Yang, W. *J. Am. Chem. Soc.* **1984**, *106*, 4049.
20. (a) Brandi, A.; Cordero, F. M.; Desarlo, F.; Gandolfi, R.; Rastelli, A.; Bagatti, M. *Tetrahedron* **1992**, *48*, 3323. (b) Coppola, B. P.; Noe, M. C.; Schwartz, D. J.; Abdon, R. L. I.; Trost, B. M. *Tetrahedron* **1994**, *50*, 93. (c) Avalos, M.; Babiano, R.; Cabanillas, A.; Cintas, P.; Jimenez, J. L.; Palacios, J. C.; Aguilar, M. A.; Corchado, J. C.; Espinosa-García, J. *J. Org. Chem.* **1996**, *61*, 7291. (d) Herrera, R.; Nagarajan, A.; Morales, M. A.; Mendez, F.; Jimenez-Vazquez, H. A.; Zepeda, L. G.; Tamariz, J. *J. Org. Chem.* **2001**, *66*, 1252.
21. Burger, K.; Albanbauer, J.; Manz, F. *Chem. Ber.* **1974**, *107*, 1823.
22. Padwa, A.; Chen, Y.-Y.; Dent, W.; Nimmegern, H. *J. Org. Chem.* **1985**, *50*, 4006.
23. Clovis, J. S.; Eckell, A.; Huisgen, R.; Sustmann, R. *Chem. Ber.* **1967**, *100*, 60.
24. (a) Becke, A. D. *J. Chem. Phys.* **1993**, *98*, 5648. (b) Lee, C.; Yang, W.; Parr, R. G. *Phys. Rev. B* **1988**, *37*, 785.
25. Hehre, W. J.; Radom, L.; Schleyer, P. v. R.; Pople, J. A. *Ab initio Molecular Orbital Theory*; Wiley: New York, 1986.
26. (a) Stanton, R. V.; Merz, K. M. *J. Chem. Phys.* **1994**, *100*, 434. (b) Carpenter, J. E.; Sosa, C. P. *J. Mol. Struct., (Theochem)* **1994**, *311*, 325. (c) Baker, J.; Muir, M.; Andzelm, J. *J. Chem. Phys.* **1995**, *102*, 2036. (d) Jursic, B.; Zdravkovski, Z. *J. Chem. Soc., Perkin Trans. 2* **1995**, 1223. (e) Goldstein, E.; Beno, B.; Houk, K. N. *J. Am. Chem. Soc.* **1996**, *118*, 6036. (f) Branchadell, V.; Font, J.; Moglioni, A. G.; Ochoa de Echaguen, C.; Oliva, A.; Ortuño, R. M.; Veciana, J.; Vidal Gancedo, J. *J. Am. Chem. Soc.* **1997**, *119*, 9992. (g) Domingo, L. R.; Arnó, M.; Andrés, J. *J. Am. Chem. Soc.* **1998**, *120*, 1617.
27. (a) Schlegel, H. B. *J. Comput. Chem.* **1982**, *3*, 214. (b) Schlegel, H. B. *Geometry Optimization on Potential Energy Surface*. In *Modern Electronic Structure Theory*; Yarkony, D. R., Ed.; World Scientific: Singapore, 1994.
28. Fukui, K. *J. Phys. Chem.* **1970**, *74*, 4161.
29. (a) González, C.; Schlegel, H. B. *J. Phys. Chem.* **1990**, *94*, 5523. (b) González, C.; Schlegel, H. B. *J. Chem. Phys.* **1991**, *95*, 5853.
30. (a) Reed, A. E.; Weinstock, R. B.; Weinhold, F. *J. Chem. Phys.* **1985**, *83*, 735. (b) Reed, A. E.; Curtiss, L. A.; Weinhold, F. *Chem. Rev.* **1988**, *88*, 899.
31. Frisch, M. J.; Trucks, G. W.; Schlegel, H. B.; Scuseria, G. E.; Robb, M. A.; Cheeseman, J. R.; Zakrzewski, V. G.; Montgomery, J. J. A.; Stratmann, R. E.; Burant, J. C.; Dapprich, S.; Millam, J. M.; Daniels, A. D.; Kudin, K. N.; Strain, M. C.; Farkas, O.; Tomasi, J.; Barone, V.; Cossi, M.; Cammi, R.; Mennucci, B.; Pomelli, C.; Adamo, C.; Clifford, S.; Ochterski, J.; Petersson, G. A.; Ayala, P. Y.; Cui, Q.; Morokuma, K.; Malick, D. K.; Rabuck, A. D.; Raghavachari, K.; Foresman, J. B.; Cioslowski, J.; Ortiz, J. V.; Stefanov, B. B.; Liu, G.; Liashenko, A.; Piskorz, P.; Komaromi, I.; Gomperts, R.; Martin, R. L.; Fox, D. J.; Keith, T.; Al-Laham, M. A.; Peng, C. Y.; Nanayakkara, A.; Challacombe, M. W.; Gill, P. M.; Johnson, B.; Chen, W.; Wong, M. W.; Andres, J. L.; Gonzalez, C.; Head-Gordon, M.; Replogle, E. S.; Pople, J. A. *Gaussian 98*, Revision A.6; Gaussian, Inc.: Pittsburgh PA, 1998.
32. (a) Parr, R. G.; Pearson, R. G. *J. Am. Chem. Soc.* **1983**, *105*, 7512. (b) Parr, R. G.; Yang, W. *Density Functional Theory of Atoms and Molecules*; Oxford University Press: New York, 1989.
33. (a) Cossío, F. P.; Morao, I.; Jiao, H.; Schleyer, P. v. R. *J. Am. Chem. Soc.* **1999**, *121*, 6737. (b) Carda, M.; Portolés, R.; Murga, J.; Uriel, S.; Marco, J. A.; Domingo, L. R.; Zaragoza, R. J.; Röper, H. *J. Org. Chem.* **2000**, 7000.
34. Wiberg, K. B. *Tetrahedron* **1968**, *24*, 1083.
35. Domingo, L. R.; Pérez, P.; Contreras, R. *Tetrahedron* **2004**, *60*, 6585.